

Mechanism of High Temperature Corrosion by Model Naphthenic Acids

Peng Jin, Winston Robbins, Gheorghe Bota
Institute for Corrosion and Multiphase Technology, Ohio University
342 West State Street
Athens, OH 45701
USA

ABSTRACT

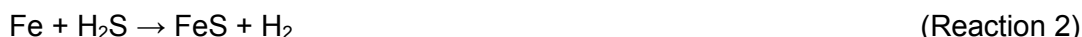
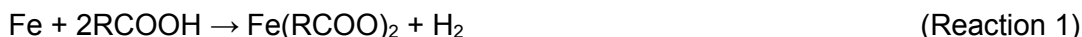
Naphthenic acid (NAP) corrosion is one of the major concerns for corrosion engineers in refineries, particularly with the increasing acidity in “opportunity crudes”. However, complex compositions of NAP in crude oil make it difficult to evaluate accurately their corrosive behavior. In the present study, several model acids, including 4-phenylbutyric acid, 1-naphthoic acid, and 4-cyclohexyl pentanoic acid, have been tested in lab scale experiments previously applied to real crude fractions. Pretreatment/challenge protocol tests the corrosive behavior of the model acids under temperature and velocity ranges close to those encountered in refineries. This work demonstrates that the pretreatment of carbon steel and 9Cr-alloy with model acids yields iron oxide scales with different morphology and chemical composition as determined by Scanning Electron Microscopy (SEM) and Transmission Electron Microscopy (TEM). It is postulated that the formation of the iron oxide scale resulted from the decomposition of iron naphthenate on the surface at high temperatures.

Key words: naphthenic acid corrosion, iron oxide, crude fractions

INTRODUCTION

Naphthenic acid (NAP) corrosion is one of the major concerns for corrosion engineers in refineries, particularly when increasing amounts of “opportunity crudes” are processed. The opportunity for these crudes is their discount of price, which often comes with higher concentrations of corrosive species, particularly NAP that may necessitate costly strategies, such as upgrading materials and adding inhibitors. The economic benefit of processing “opportunity crudes” must be balanced against the problem of corrosion. Therefore, there is a strong incentive to study the fundamentals of NAP corrosion.¹

NAP generally refers to the natural carboxylic acids in petroleum. These acids typically contain one or more one five- or six-member rings. In the refinery, NAP corrosion is accompanied by corrosion from reactive sulfur compounds (that may form H₂S). High-temperature corrosion of steel is commonly represented by the following reactions:²



In Reaction 1, NAP (RCOOH) reacts to form iron naphthenate [Fe(RCOO)₂] that is oil soluble. At high temperatures, sulfur compounds in the crude may decompose to H₂S and corrode the steel, as shown in Reaction 2. As the corrosion product, FeS (iron sulfide) is not oil soluble and grows as a scale on the steel surface. It is generally accepted that the iron sulfide scale is somewhat protective acting as a permeation barrier, but conditions that contribute to its formation and stability are not well understood. In our prior research with model NAP and a sulfur compound in a pretreatment/challenge experiment, it was found that a protective scale of magnetite (Fe₃O₄) was formed under the sulfide layer.³ The magnetite scale was formed on the steel surface during the corrosion by a commercial NAP mixture. It was also found that the presence of chromium improved the protectiveness of scale. It has been hypothesized that the iron naphthenate undergoes decomposition at the high pretreatment temperatures as shown in Reactions 4&5.



The magnetite scale in our prior research was formed by a complex mixture of NAP. The formation of magnetite and its protectiveness varied among samples. The molecular structures of the reactive acids were unknown. Molecular structure has been previously investigated for its effect in laboratory corrosion experiment.⁴ Structural shape and molecular weight (MW) were noted to affect corrosion rates in some cases. Iron naphthenates were recognized as being less thermally stable than the parent acids which accounted for losses of iron naphthenate from solution in iron powder tests. However, in those studies no mention is made of magnetite scale formation.

In order to investigate the effect of molecular structure of acid on the corrosion and formation of protective magnetite scales, three representative model acids (4-phenyl butyric acid [PBA], 4-cyclohexyl pentanoic acid [CxPA], and 1-naphthoic acid [NA]) were employed to generate the corrosion product scale. Each of model acids was mixed in a model inert mineral oil to pretreat steel specimens in an autoclave. In order to study the protectiveness, the corrosion product scale was challenged by a solution of commercial NAP in a rotating cylinder autoclave reactor.

EXPERIMENTAL PROCEDURE

Experimental Materials

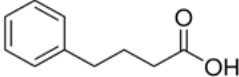
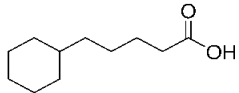
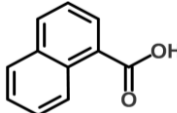
Two of commonly utilized steels in refineries were selected for experimentation, i.e., the UNS K03006 carbon steel (CS) and UNS S50400 steel (9Cr). Steel specimens were machined in the shape of rings with inner diameter 70.43 mm (2.77 in), outer diameter 81.76 mm (3.22 in), and thickness 5 mm (0.20 in). Before experiments, each ring was polished with 400 and 600-grit silicon-carbide paper (SiC) in succession. Rings were polished under the flow of isopropanol to prevent oxidation and overheating.

After polishing, rings were wiped with a paper towel, rinsed with toluene and acetone, and dried with nitrogen flow. Weights of fresh polished rings were taken with an analytical balance.

Experimental Solutions

All solutions were made in a high boiling white mineral oil processed to eliminate all heteroatoms. Each model acid (PBA, CxPA, or NA) was dissolved in the mineral oil to prepare the experimental solutions used to pretreat steel rings (Table 1). In PBA and CxPA, the carboxylic group is separated from the ring by 3 (PBA) or 4 (CxPA) CH₂ groups; in NA the acid group is attached directly to the aromatic ring. Each of these structure differs somewhat from indigenous NAP in crudes where a -CH₂COOH resides on a saturated ring. These acids that each had a boiling point close to pretreatment condition were investigated for the effect of their structures on scale formation.

Table 1. Model acids in the pretreatment of rings

	Experimental solutions with model acids	Structure of acid	TAN	S%	Acid boiling point
PBA	4-Phenyl butyric acid + mineral oil		1.75	0	340°C (644°F)
CxPA	4-Cyclohexyl pentanoic acid + mineral oil		1.75	0	331°C (628°F)
NA	Naphthoic acid + mineral oil		1.75	0	300°C (572°F)

Physical and chemical properties of the mineral oil can be found in our prior publication.³

Experimental Equipment

The pretreatment/challenge protocol used two different experimental setups:

- 1) A closed stirred autoclave where rings were pretreated with one of the experimental solutions at high temperature. The experimental solution was stirred continuously while rings were stagnant.
- 2) A flow-through rotating cylinder autoclave called the High Velocity Rig (HVR) was used to investigate the scale protectiveness against NAP corrosion under high temperature and high velocity conditions. (**Figure 1**).

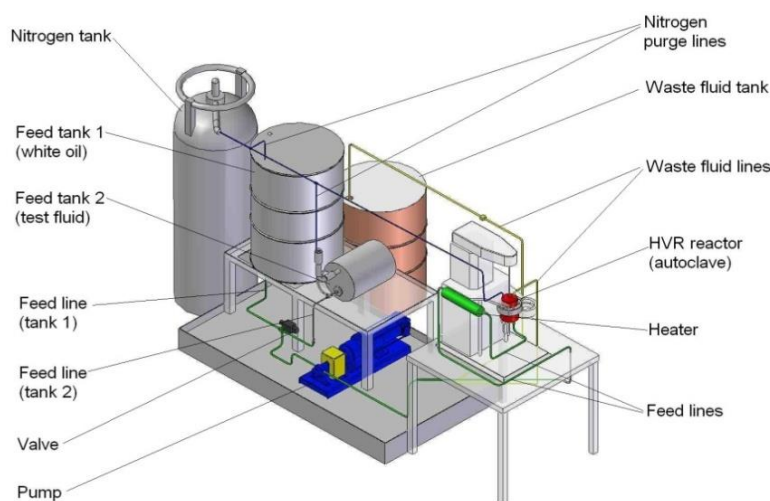


Figure 1. Schematic rendering of the High Velocity Rig (HVR) used in the “challenge” experiment.

Experimental Procedures

Two parallel experiments were performed for each acid using a set of three CS/9Cr rings. In the first experiment the rings were pretreated only to determine the corrosion rates and formation of scale. In the second, pretreatment was followed by a challenge to determine the protectiveness of any scale against a more severe corrosion condition. “*Pretreatment*” of CS and 9Cr rings was carried out at 316°C (600°F) in the autoclave for 24 hours.

“*Pretreatment - Challenge*” was performed on CS and 9Cr rings transferred after 600°F pretreatment with their scale intact onto a cylinder in the HVR. The HVR was fed with the challenge solution - commercial NAP in mineral oil (TAN = 3.5, S = 0%wt) - at a flow rate of 7.5 cm³/min for 24 h at 343°C (650°F) while rings on the cylinder were rotated at 2000 rpm (equivalent to a peripheral velocity of 8.5 m/s, Reynolds number of 1771 and wall shear stress of 74 Pa). A back-pressure of 1.1×10⁶ Pa (150 psig) was applied to suppress breakout of gas.

Weight losses were determined for two rings of each alloy at the end of both the pretreatment and at the end of the pretreatment-challenge experiments. In both cases, the rings were rinsed under the flow of toluene and acetone successively, rubbed with a brush, and treated with “Clarke” solution to constant weight as determined with an analytical balance per ASTM G1 - 03.^{5,6} Corrosion rates were calculated based on the weight loss and surface area.

In each experiment, the third ring of each alloy was used to investigate morphology and chemical composition of the scales using a Scanning Electron Microscope - SEM and Focused Ion Beam / Transmittance Electron Microscope – FIB/TEM combined with energy dispersive X-ray spectroscopy (EDS) as well as X-Ray Diffraction (XRD).

Evaluation of Corrosion Rates

Corrosion rates of rings were calculated based on their weight loss during the experiment. For the pretreatment experiment conducted in the autoclave, the corrosion rate was calculated using Equation (1).

$$CR_{Pretreatment} = \frac{(IW - FW)}{\rho_{steel} \times A_s \times t} \times 10 \times 24 \times 365 \quad (1)$$

where:

$CR_{Pretreatment}$ – Pretreatment corrosion rate, [mm/y]

IW – Initial weight of fresh polished ring, [g]

FW – Final weight of ring after treated with Clarke solution, [g]

ρ_{steel} – Density of ring, [g/cm³]

$A_{s, Pretreatment}$ – Area of ring exposed to corrosive fluid during pretreatment, [cm²]

$t_{Pretreatment}$ – Duration of experimentation in the stirred autoclave, [h]

In the pretreatment-challenge step, fresh polished rings were pretreated in the autoclave followed by challenging in the HVR. While the corrosion rate in the pretreatment step could be calculated according to Equation (1), the challenge corrosion was assessed by using the following equation.

$$CR_{Challenge} = \frac{(IW - FW - WL_{Pretreatment})}{\rho_{steel} \times A_s \times t} \times 10 \times 24 \times 365 \quad (2)$$

where:

$CR_{Challenge}$ – Net Corrosion rate from the challenge phase (excluding the autoclave phase), [mm/y]

IW – Initial weight of fresh polished ring, [g]

FW – Final weight of ring after treated with Clarke solution, [g]

$WL_{Pretreatment}$ – Weight loss of ring in the pretreatment phase, [g]

ρ_{steel} – Density of ring, [g/cm³]

$A_{s, Challenge}$ – Area of ring exposed to corrosive fluid during challenge, [cm²]

$t_{Challenge}$ – Duration of experimentation in the HVR, [h]

RESULTS

Following sections present and discuss the experimental data for model acids. They are divided into the following sections: Effect of Acid Structure; Effect of Temperature; Structure of Oxide Scale.

Effect of Acid Structure

Corrosion rates for CS rings pretreated in PBA, CxPA, and NA at TAN 1.75 are shown in Figure 2. The 316°C (600°F) pretreatment corrosion rates are low and close to one another. However, the challenge corrosion rates vary. Pretreatment in CxPA and NA lowers the challenge corrosion rates slightly below that for pure TAN 3.5 corrosion rate (Pure TAN 3.5 corrosion rate refers to the HVR challenge corrosion rate of freshly polished rings (without pretreatment) at TAN 3.5). The slight changes suggest that no protective scale was formed by the CxPA or NA pretreatment. On the other hand, pretreatment in PBA appears effective in reducing corrosion in the challenge, suggesting that scale formation may have occurred.

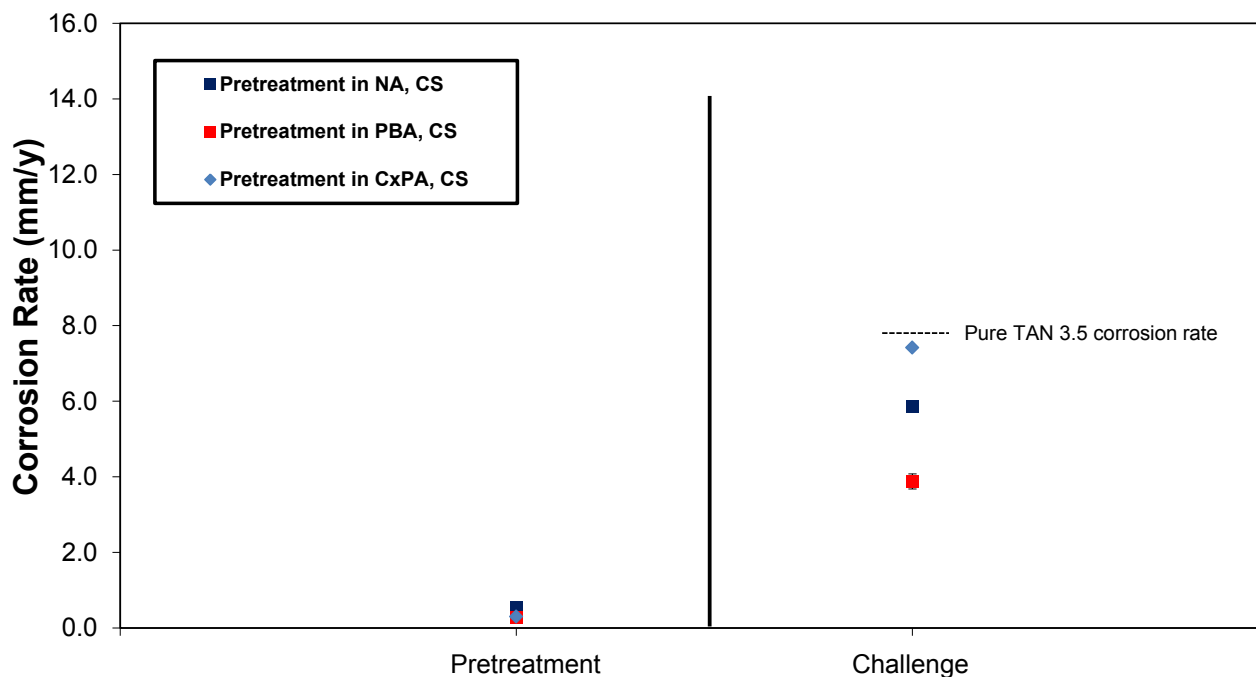


Figure 2. Pretreatment and challenge corrosion rates of CS rings pretreated in PBA, CxPA, and NA in white mineral oil.

Plain-view SEM/EDS analysis of the CS rings is shown in Figure 3. A continuous scale is observed on the ring surface pretreated in PBA (image a) or CxPA (image b). EDS analysis reveals that the scale is composed of iron and oxygen. On the other hand, the pretreatment in NA resulted in a surface with isolated particles rather than a continuous scale (image c). No oxygen is detected in the EDS analysis which suggests that the NA did not promote the formation of a continuous oxide scale.

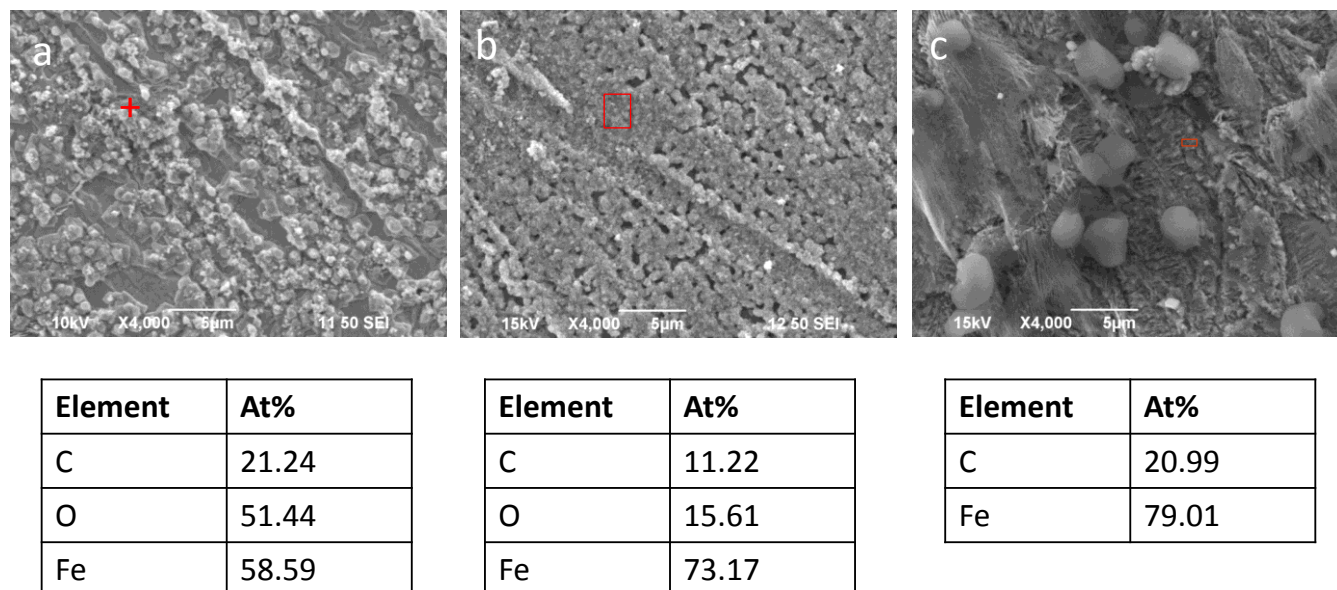


Figure 3. Plain-view SEM and EDS analysis of CS rings pretreated in PBA (a), CxPA (b), and NA (c) in mineral oil (The EDS analysis was performed in the red areas shown in the SEM images).

The corresponding cross-section SEM images of scales formed in PBA and EDS scanning analysis shows a broad peak of oxygen adjacent to the steel surface (images a and a' of Figure 4). The scale formed in with CxPA is also quite thin and EDS analysis indicates the presence of oxygen (images b and b'). Cross-section SEM image of the steel pretreated in NA (image c) reveals an isolated area composed of iron and oxide rather than a continuous scale, which is consistent with the findings of plain-view SEM/EDS analysis. It suggests that NA did not effectively promote the formation of a robust oxide scale.

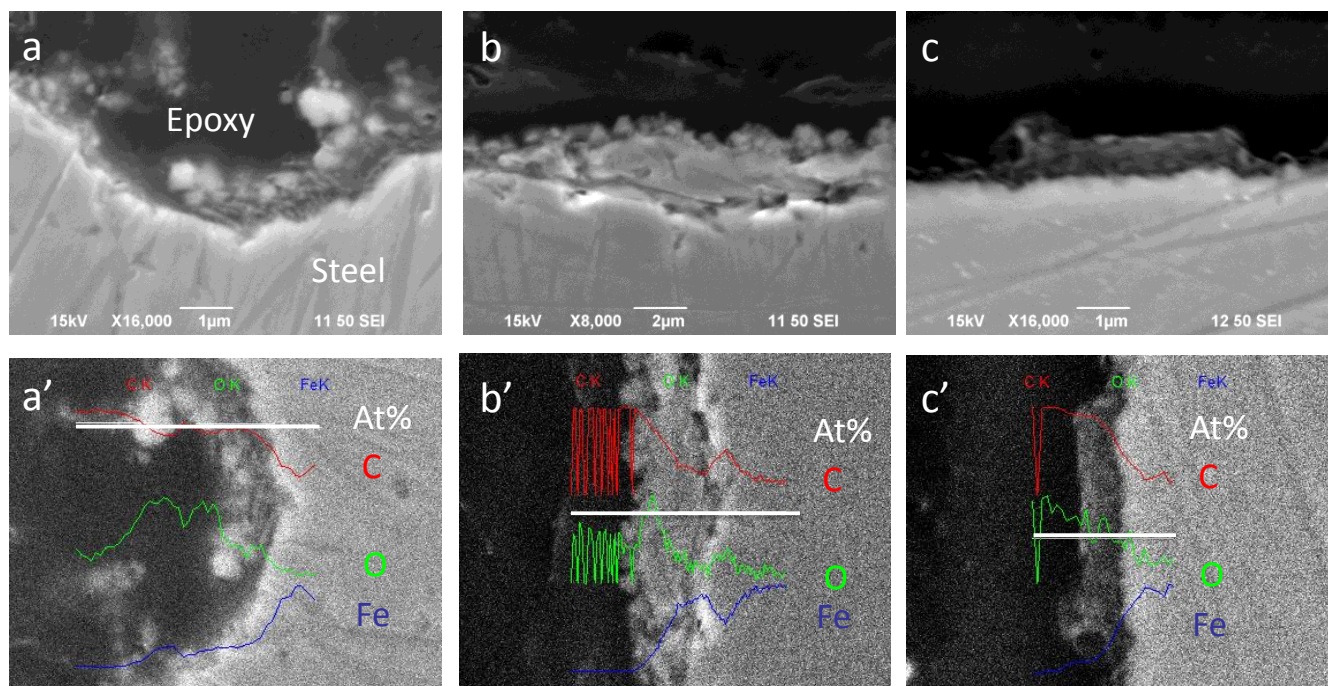


Figure 4. Cross-section SEM analysis of CS ring pretreated in PBA (a), CxPA (b), and NA (c) in mineral oil. The EDS analysis was performed along the white line in images a', b', and c'.

After the challenge by the TAN 3.5 solution, the plain-view SEM shows that the scale on the CS ring has picked up a minor amount of sulfur (Figure 5a), although oxygen is still the major nonmetal element. Similar phenomena are also observed for the CS rings pretreated in CxPA. The presence of sulfur in the outer scales can be attributed to trace sulfur content in the commercial NAP. Challenge of the CS rings pretreated with NA results in a delaminated scale and the major component detected at the EDS spot is iron.

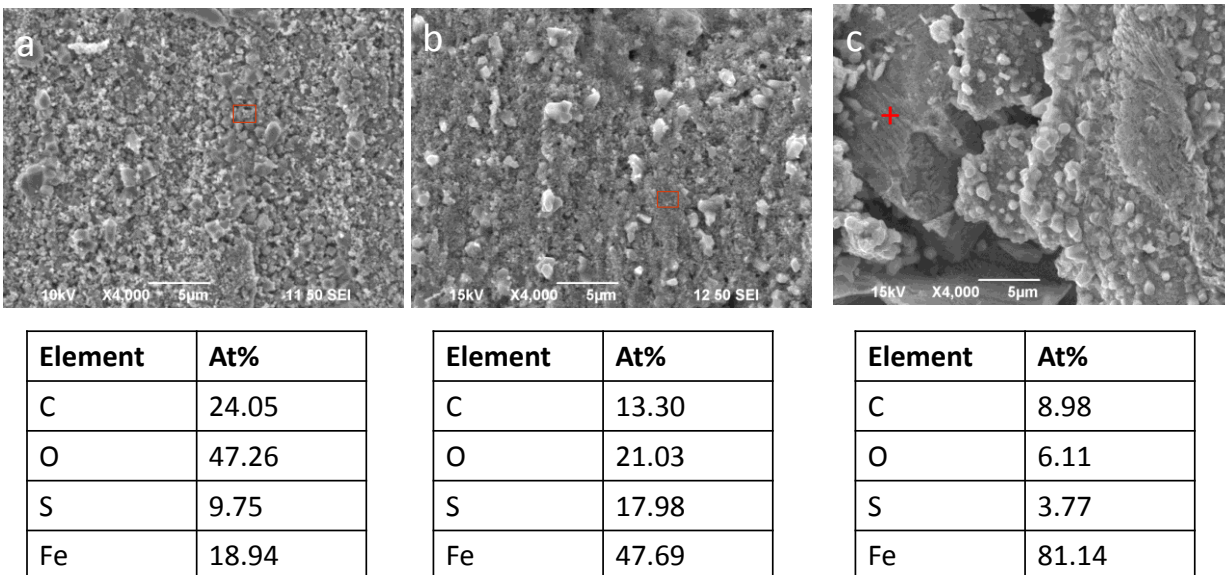


Figure 5. Surface SEM and EDS analysis of CS rings pretreated in PBA (a), CxPA (b), and NA (c) in mineral oil after TAN 3.5 challenge (The EDS analysis was performed in the red areas shown in the SEM images).

The corresponding cross-section SEM analyses show that detached scales are formed on CS rings for all three acid pretreatments after the challenge (Figure 6). These results suggest that the commercial NAP in the challenge solution can diffuse or dissolve the thin oxide scales seen in Figure 4 and corrode the underneath ferritic iron in the steel leaving pillars of pearlite under the sulfide layer, given that challenge corrosion rates for all three acid pretreatments are higher than 3 mm/y (118 mpy). For PBA and CxPA, the challenge corrosion rates are retarded slightly by the continuous oxide scale while the NA offers little resistance because it lacks a continuous scale of the oxide.

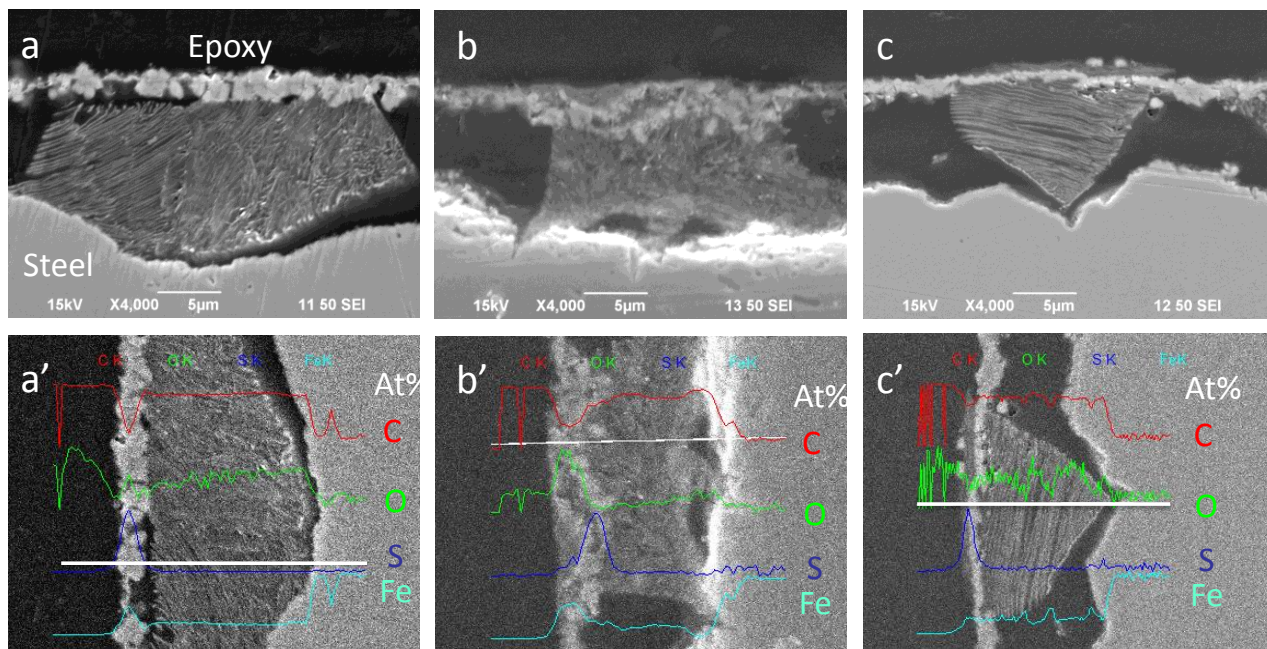


Figure 6. Cross-section SEM analysis of CS rings pretreated in (PBA (a), CxPA (b), and NA (c) in mineral oil after TAN 3.5 challenge (The EDS analysis was performed along the white line in images a', b', and c').

Pretreatment and challenge corrosion rates of 9Cr rings are shown in Figure 7. Not surprisingly, the 9Cr pretreatment corrosion rates are lower than those for CS (note lower corrosion rate scale). In this case, PBA is less corrosive than the other two acids in pretreatment. The pretreatment in PBA or CxPA leads to a low challenge corrosion rate, suggesting the formation of protective scale.

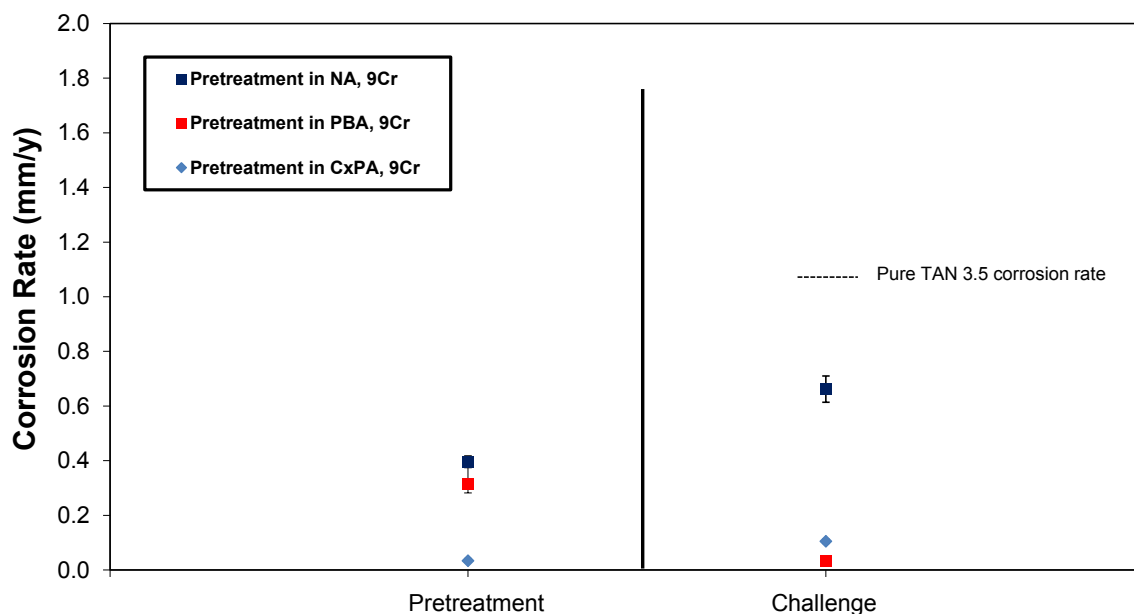


Figure 7. Pretreatment and challenge corrosion rates of 9Cr rings pretreated in PBA (a), CxPA (b), and NA (c) in mineral oil.

The plain-view SEM/EDS analysis is shown in Figure 8. The polishing marks are still visible on all 9Cr rings after pretreatment. Oxygen is present on 9Cr rings pretreated in PBA (a), CxPA (b), and not on the surface exposed to NA, which is consistent with the observation for CS rings.

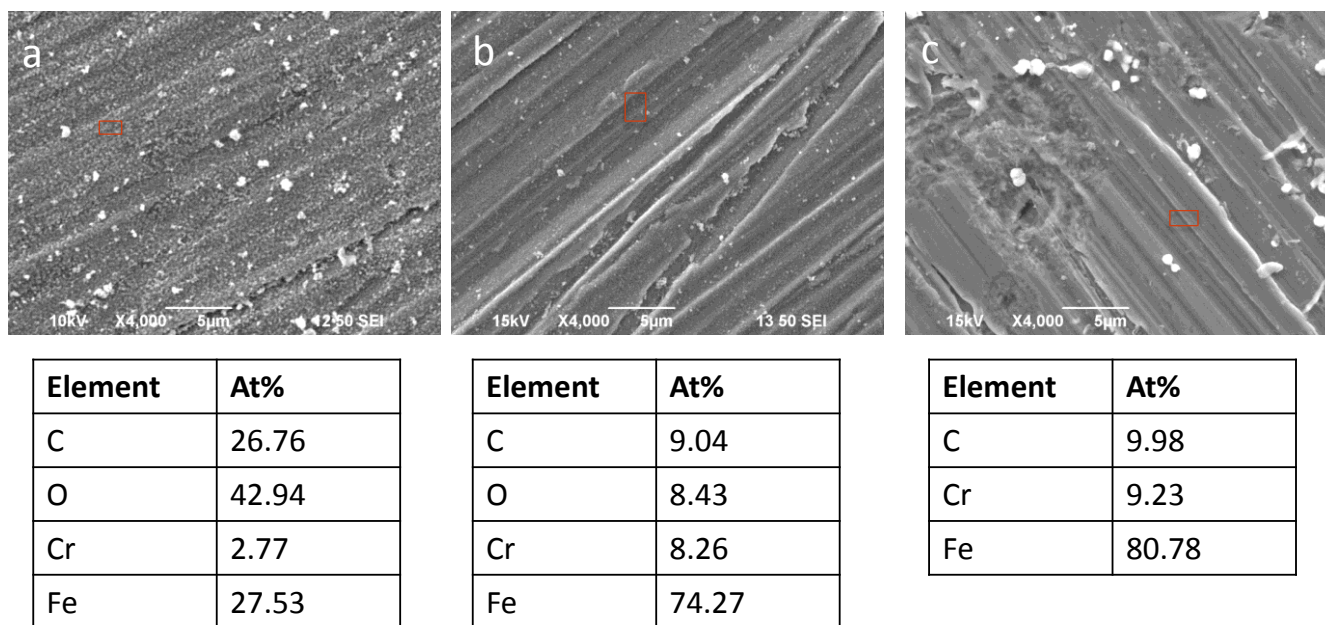


Figure 8. Plain-view SEM and EDS analysis of 9Cr rings pretreated in PBA (a), CxPA (b), and NA (c) in mineral oil. The EDS analysis was performed in the red areas shown in the SEM images.

The cross-section SEM images in Figure 9 show blurred interfaces between the epoxy and the steel for all three pretreatment solutions cases, which hinder a clear observation of scales morphology. The peak of oxygen in the EDS analysis may indicate the presence of an oxide scale, but the resolution of SEM images is not high enough for any conclusive evidence.

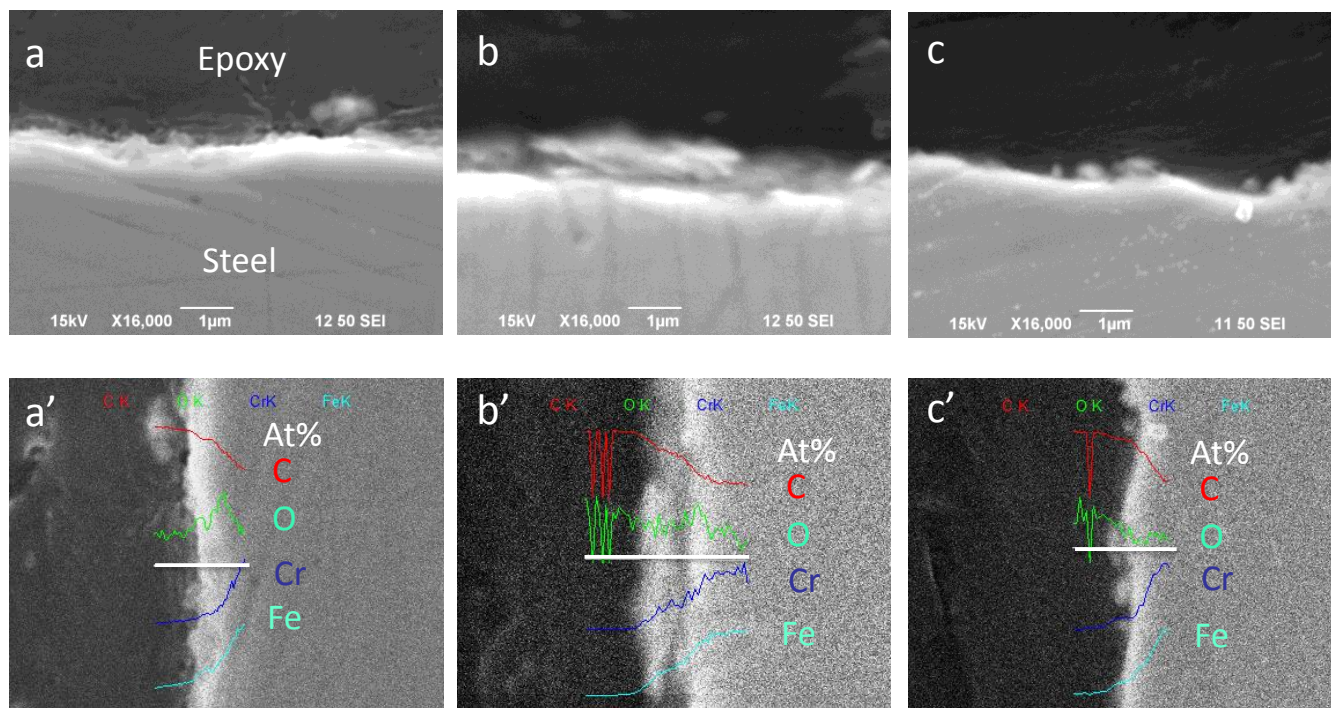


Figure 9. Cross-section SEM analysis of 9Cr rings pretreated in PBA (a), CxPA (b), and NA (c) in mineral oil (The EDS analysis was performed along the white line in images a', b', and c').

For 9Cr rings pretreated in PBA or CxPA, the surface morphology does not change significantly after the challenge by TAN 3.5 solution (images a and b in Figure 10), given the low challenge corrosion rates. On these rings, polishing marks are still visible and oxygen is also present. For the 9Cr ring pretreated in NA, the TAN 3.5 solution in the challenge removes polishing marks and leaves the oxygen on the steel surface (images c in Figure 10). Cross-section SEM/EDS analysis (Figure 11) clearly shows that oxide scales are formed on all 9Cr rings after the challenge.

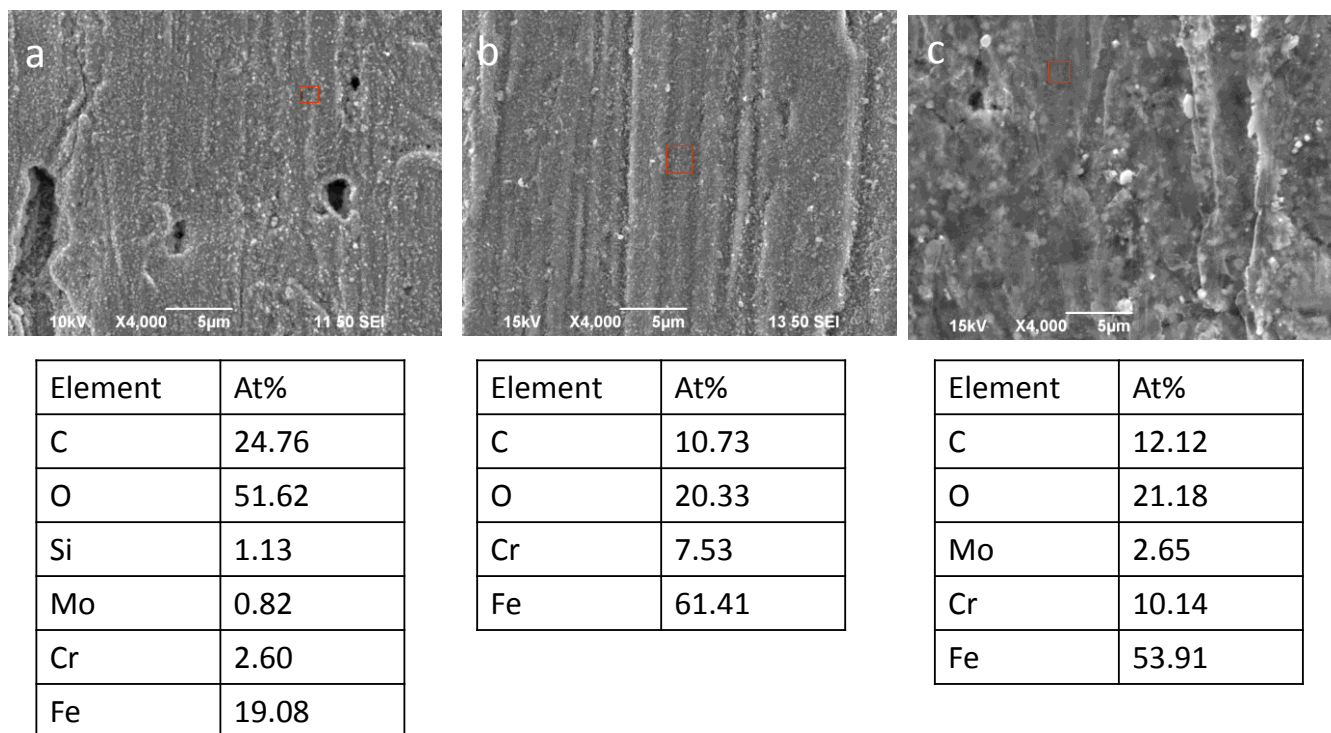


Figure 10. Surface SEM and EDS analysis of 9Cr rings pretreated in PBA (a), CxPA (b), and NA (c) in mineral oil after challenge by TAN 3.5 solution (The EDS analysis was performed in the red areas shown in the SEM images).

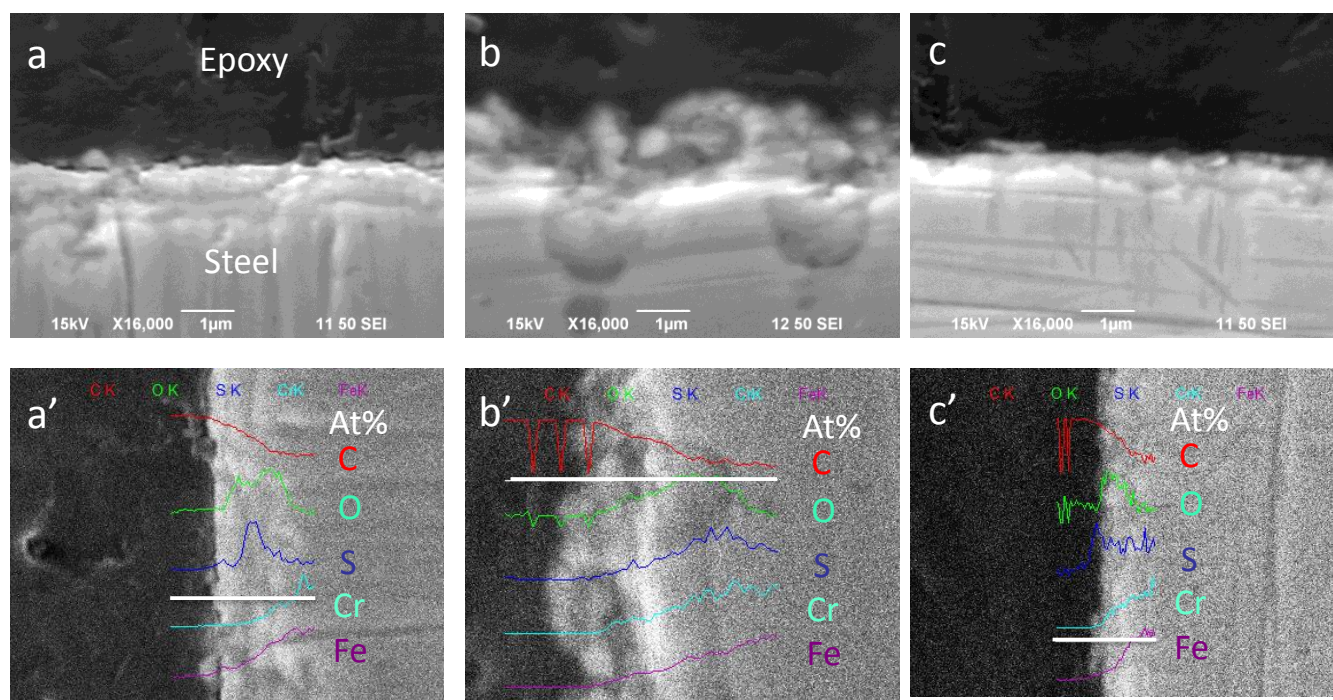


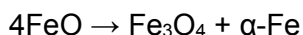
Figure 11. Cross-section SEM analysis of 9Cr rings pretreated in PBA (a), CxPA (b), and NA (c) in mineral oil after challenge by TAN 3.5 solution (The EDS analysis was performed along the white line in images a', b', and c').

As a summary, the oxide scale formed by PBA at 600°F is the most effective in deterring the corrosion during the challenge by naphthenic acids. NA is the least effective of the three selected model acids in the formation of oxide scale. The challenge corrosion rates after NA pretreatment is close to the pure

TAN 3.5 corrosion rate (for both CS and 9Cr). This suggests that $-\text{CH}_2\text{COOH}$ of longer separation between the ring and the carboxyl group favors the formation of oxide scale. But the resolution of SEM images is not high enough to reveal the structure of the oxide scale.

Effect of Temperature

It is hypothesized that the formation of oxide scale is due to the decomposition of iron naphthenates at the high corrosion temperatures.⁷



To determine if lowering the pretreatment temperature affected the oxide scale formation, rings were pretreated in PBA at 288°C (550°F) and then challenged as before. The scale formed with PBA at 288°C (550°F) was thinner and more granular than the one formed at 316°C (600°F). However, corrosion rates and SEM analyses were very similar to those for the 316°C (600°F) PBA pretreatment (data not shown). Thus, the lower temperature did not affect the marginal protectiveness of the oxide scale generated by the PBA.

Structure of Oxide Scale

High-resolution TEM was used to get better resolution of oxide scale formed with PBA on CS rings and XRD was used to determine its crystal structure.

The TEM image of CS pretreated in PBA detects a thin scale (Figure 12) and EDS mapping confirms that the scale is composed of oxygen and iron (Figure 13). The TEM image and its corresponding mapping analysis also show that there are some white areas in the scale which are deficit in oxygen but rich in carbon. This suggests that some cementite (Fe_3C) is not corroded by PBA. The EDS line scanning (Figure 14) shows that the oxygen accounts to about 60% in the scale, which is consistent with the finding of Fe_3O_4 in the XRD analysis (Figure 15).

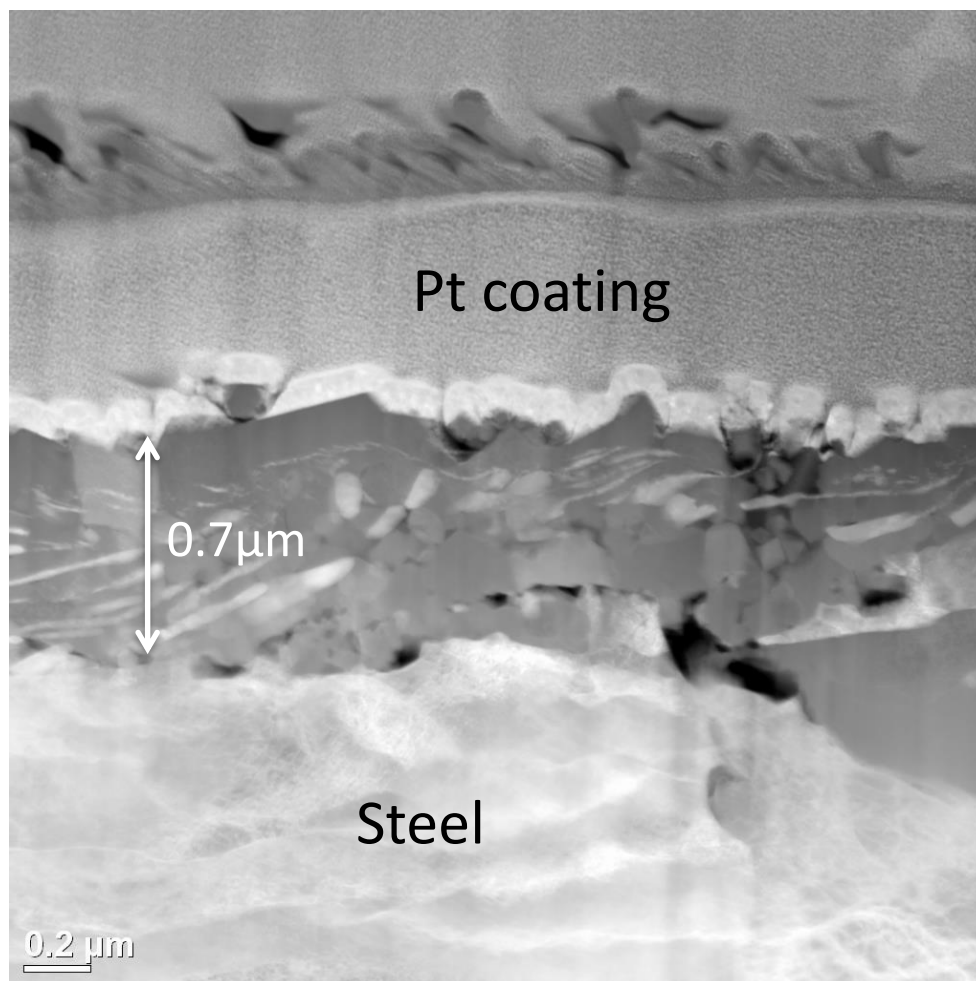


Figure 12. TEM image of CS rings pretreated in PBA in mineral oil at 316°C (600°F).

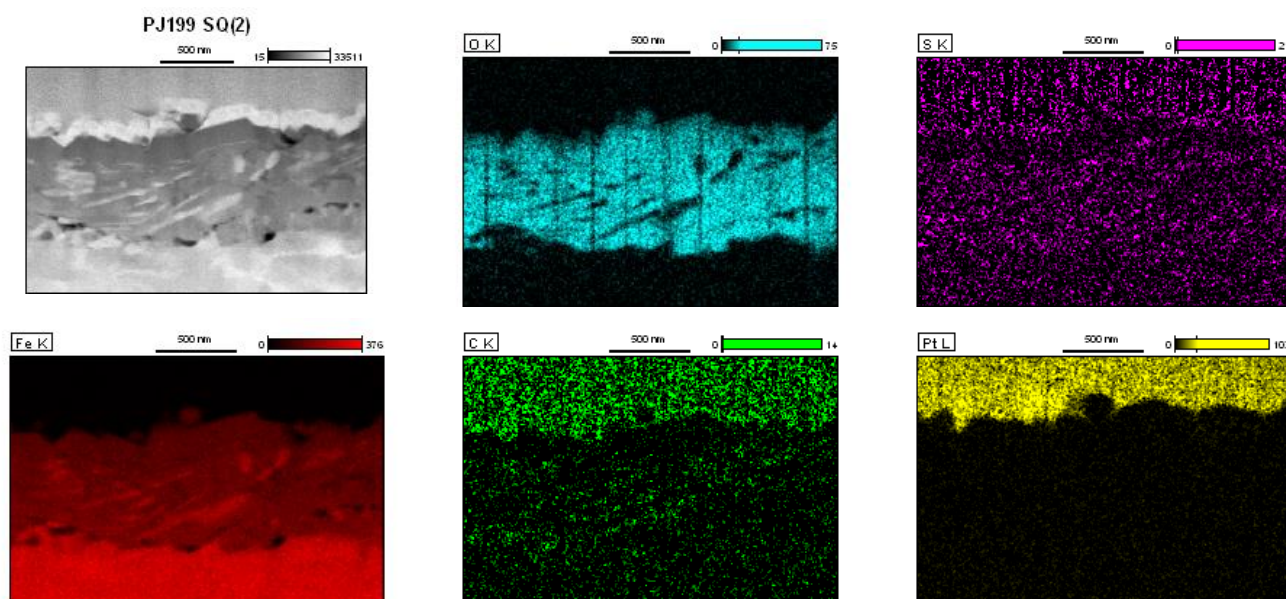


Figure 13. EDS mapping of CS rings pretreated in PBA in mineral oil at 316°C (600°F).

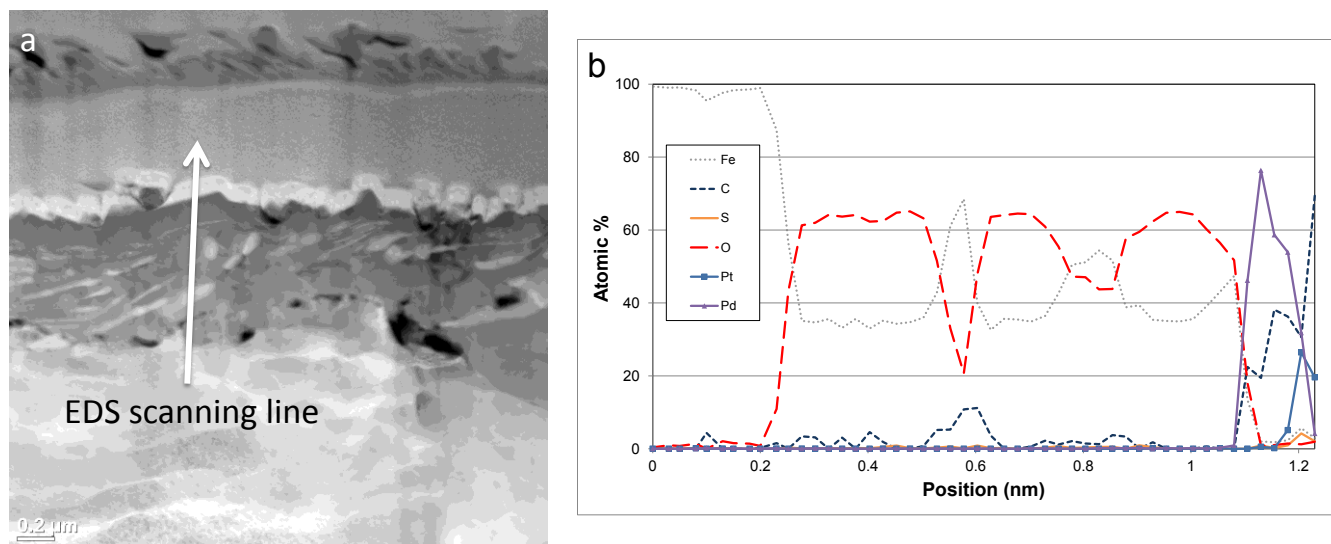


Figure 14. Elemental profile of the scale on CS rings pretreated in PBA in mineral oil at 316°C (600°F). (a) Image of the scale with the line of EDS scanning; (b) Results of EDS analysis.

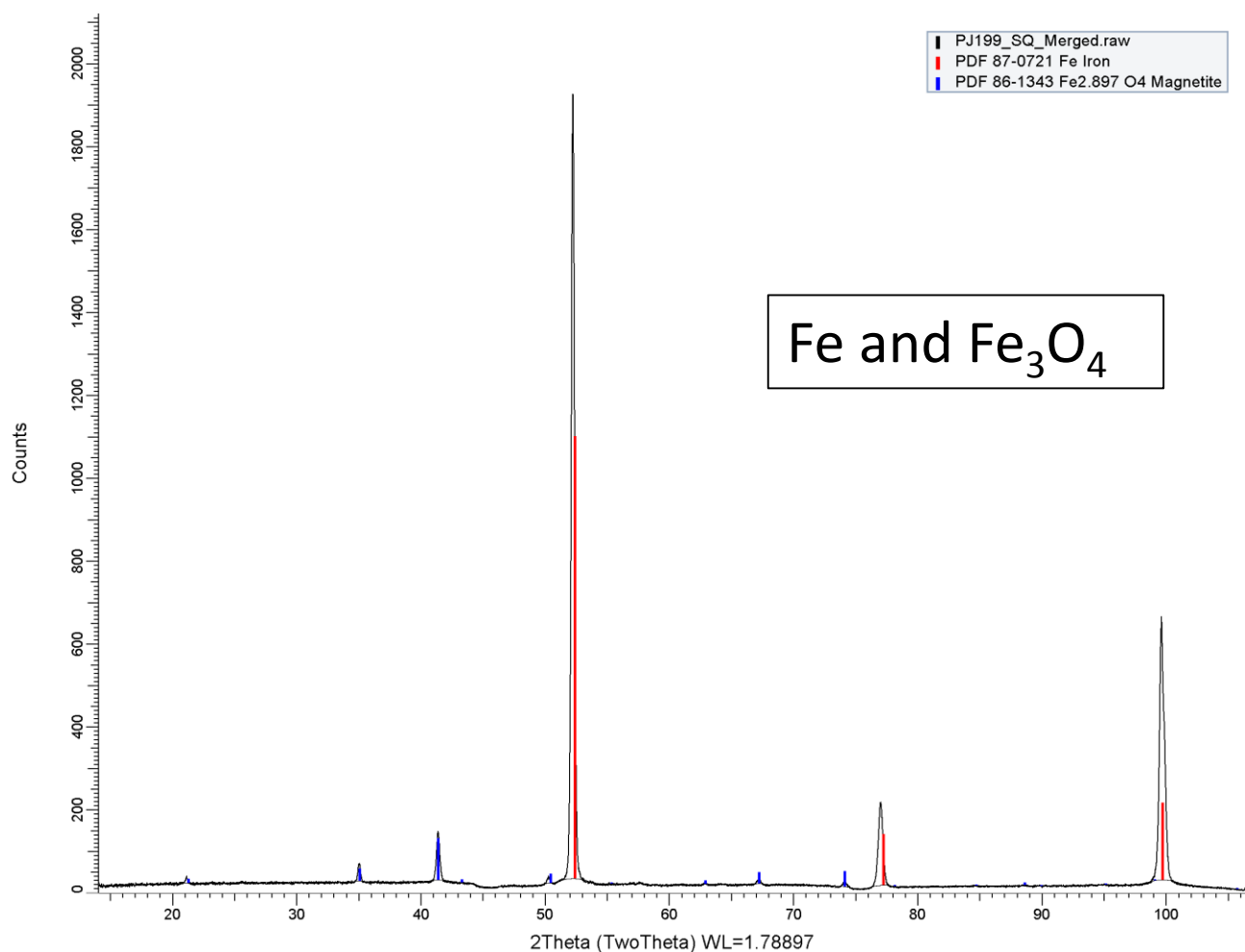


Figure 15. XRD analysis of the scale on CS rings pretreated in PBA in mineral oil at 316°C (600°F).

TEM on the ring after the challenge shows that most of the oxide scale is removed by the challenge solution of TAN 3.5 (Figure 16) and EDS mapping only detects isolated oxide particles (Figure 17).

XRD analysis confirms the presence of magnetite (Fe_3O_4) (Figure 18). The troilite (FeS) may be formed due to the sulfur content in the commercial NAP.

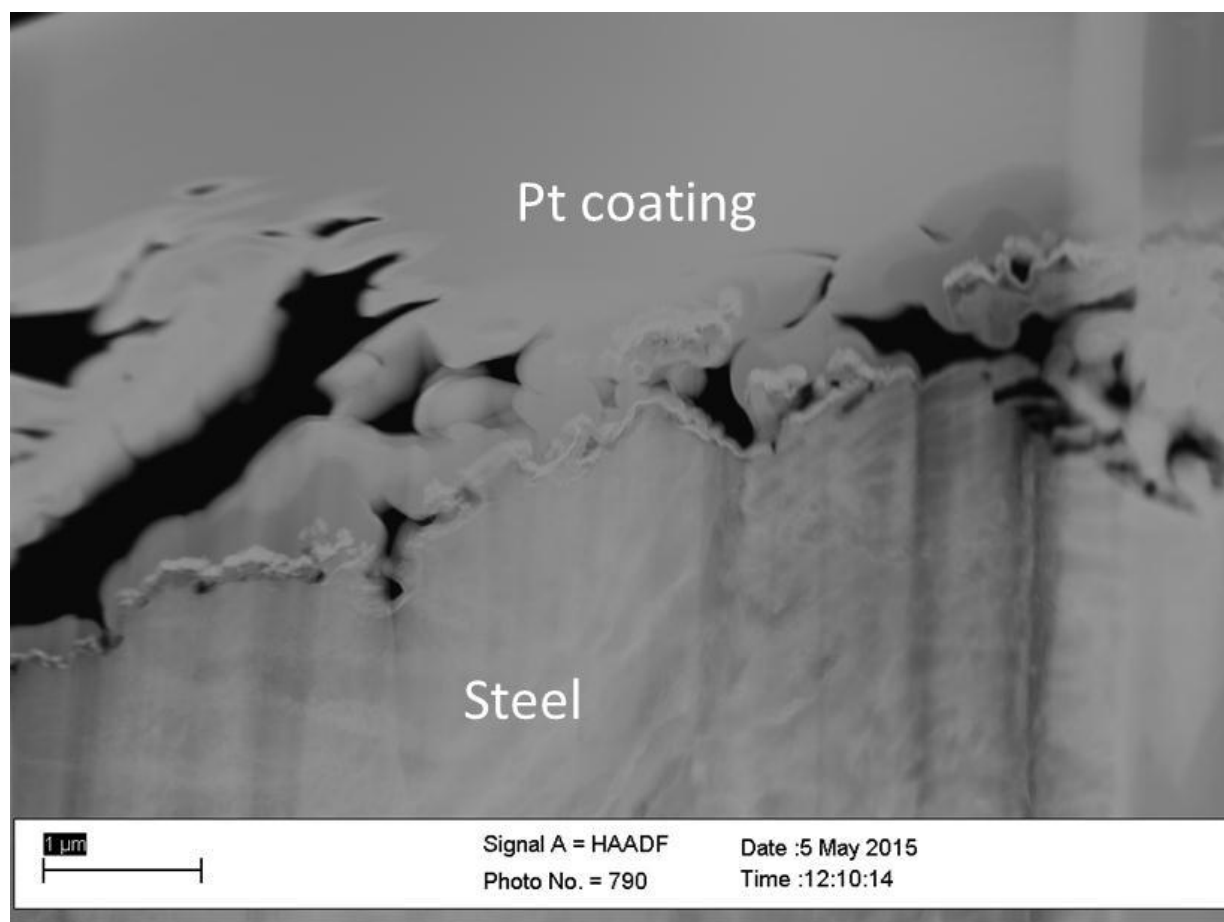


Figure 16. TEM image of CS rings pretreated in PBA in mineral oil at 316°C (600°F) after challenge by TAN 3.5 solution.

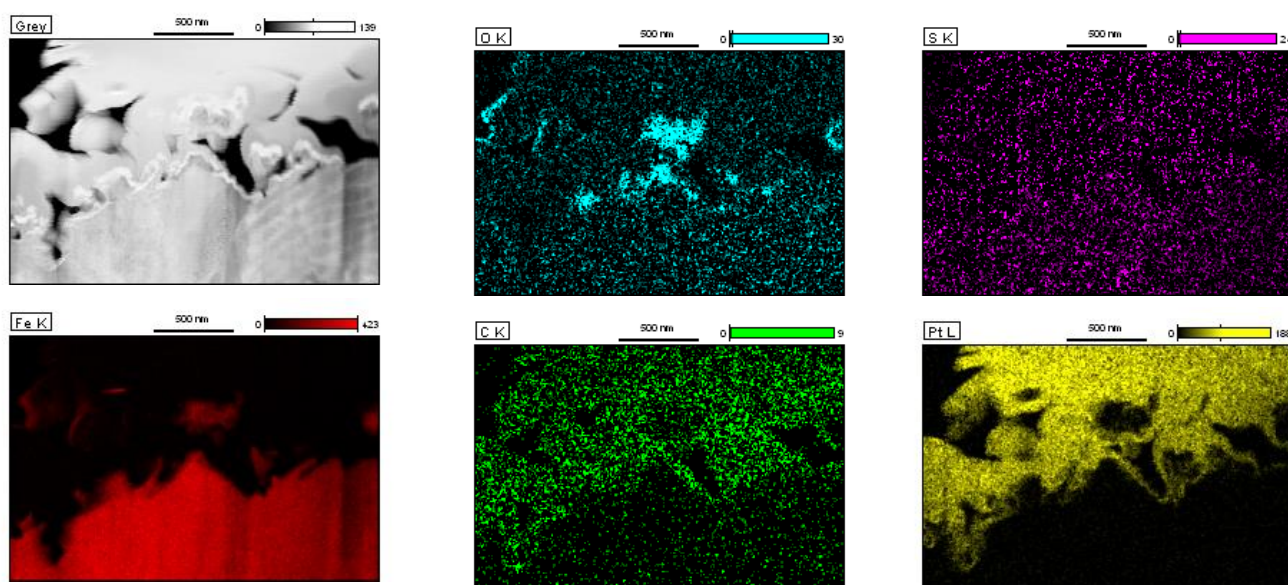


Figure 17. EDS mapping of CS rings pretreated in PBA in mineral oil at 316°C (600°F) after challenged by TAN 3.5 solution.

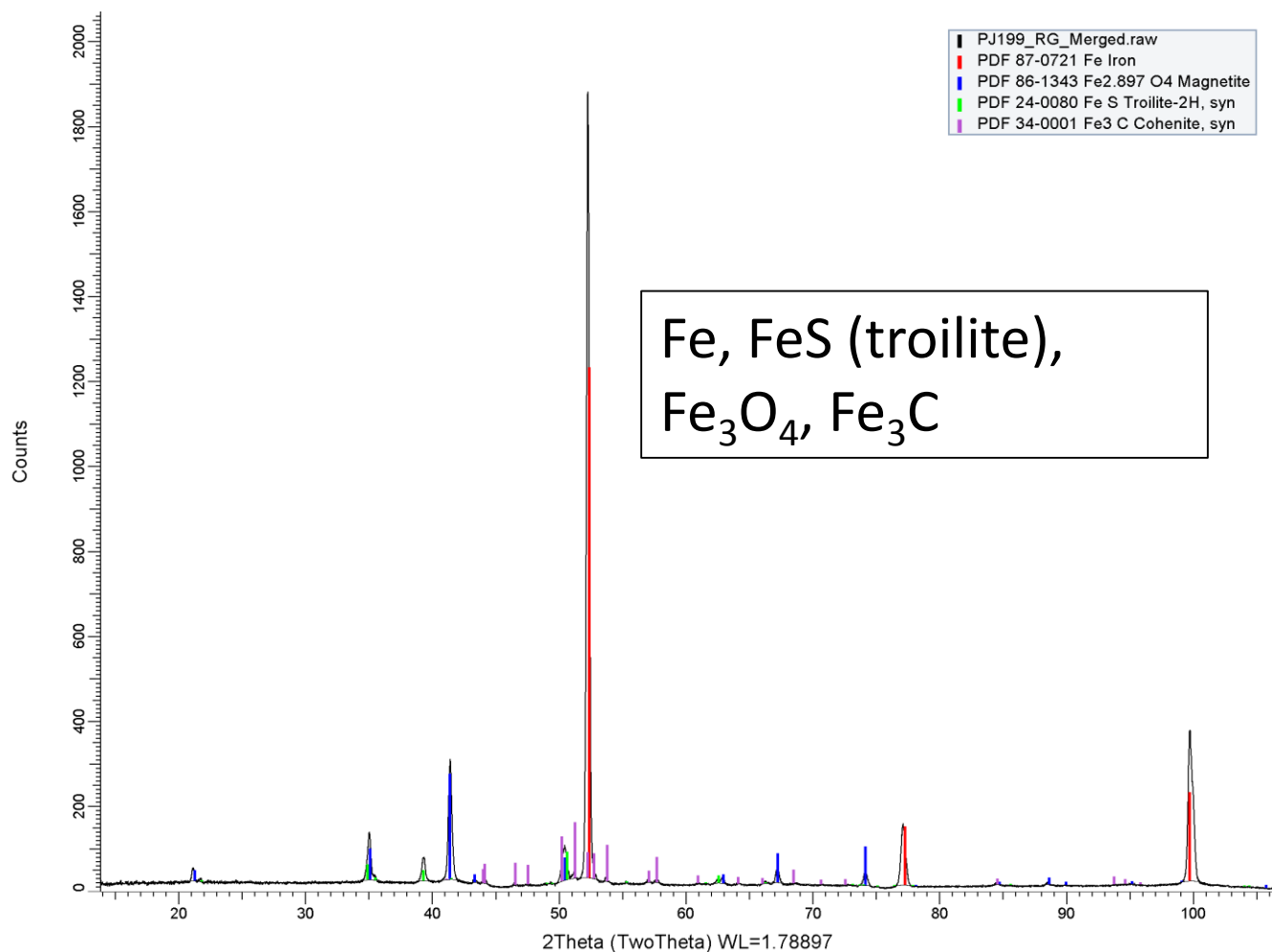


Figure 18. XRD analysis of the scale on CS rings pretreated in PBA in mineral oil at 316°C (600°F) after challenge by TAN 3.5 solution.

The scale formed in PBA pretreatment at 288°C (550°F) shows larger particles with gaps between them (Figure 19). EDS mapping (Figure 20) demonstrates that the scale is composed of iron oxide, possibly with some cementite (Fe₃C) buried within, as suggested by the EDS line scanning (Figure 21).

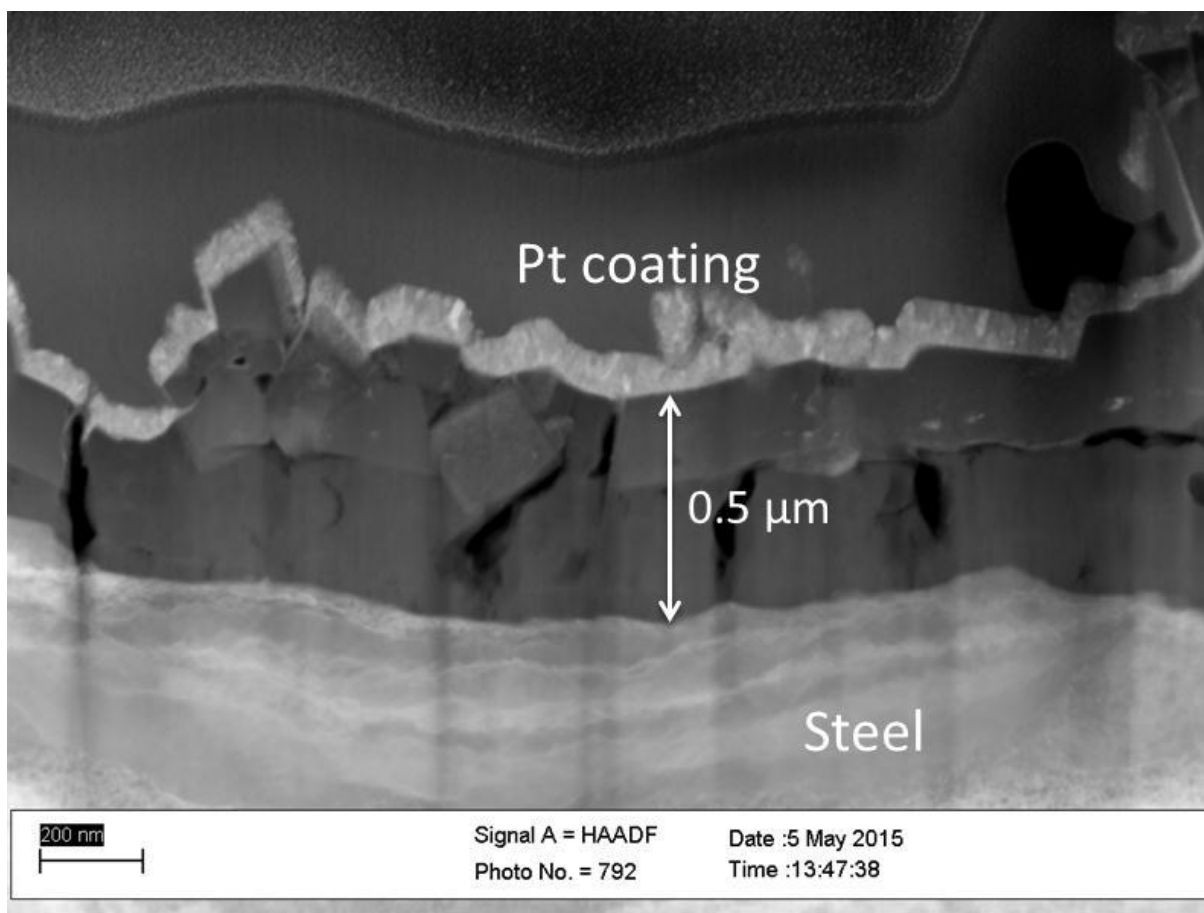


Figure 19. TEM image of CS rings pretreated in PBA in mineral oil at 288°C (550°F).

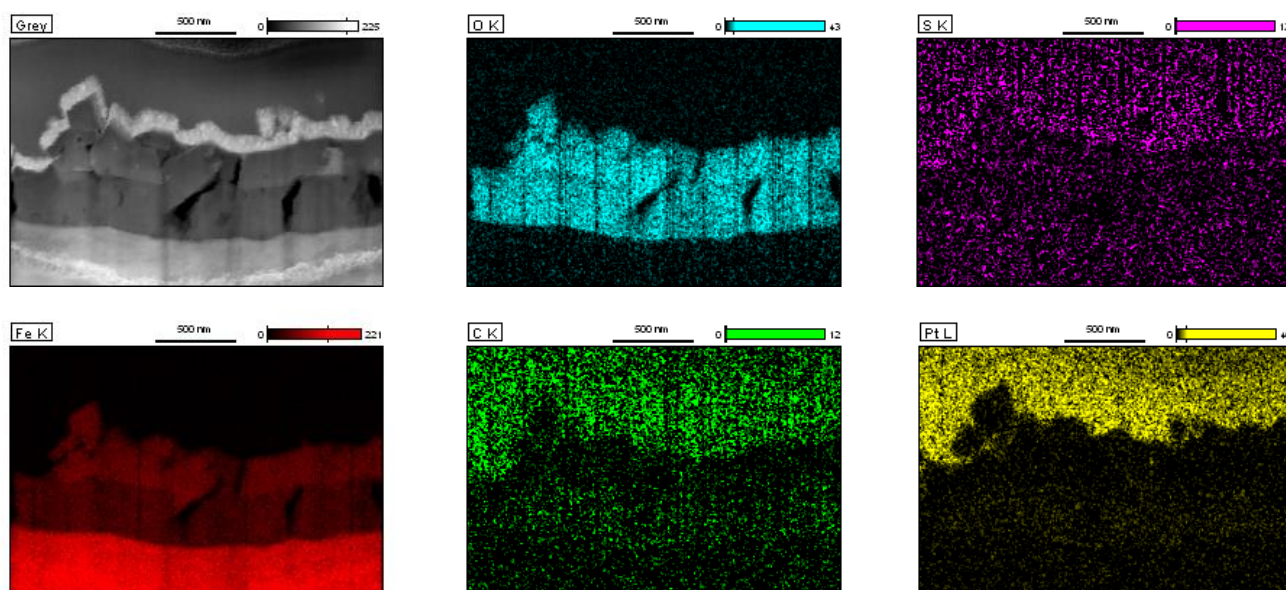


Figure 20. EDS mapping of CS rings pretreated in in PBA in mineral oil at 288°C (550°F).

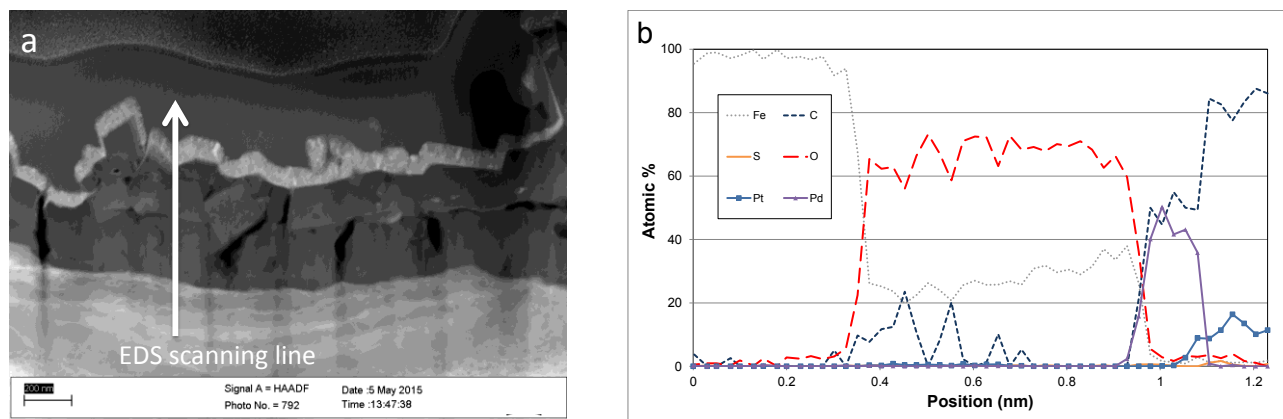


Figure 21. Elemental profile of the scale on CS rings pretreated in PBA in mineral oil 288°C (550°F). (a) Image of the scale with the line of EDS scanning; (b) Results of EDS analysis.

CONCLUSIONS

These studies reveal that autoclave pretreatment at 316°C (600°F) of rings produced thin weakly adherent oxide scales. Of the three model compounds tested, PBA produced the scale with the greatest resistance to corrosion when challenged with higher severity (TAN 3.5/343°C (650°F)) in the flow through HVR. SEM revealed that the PBA pretreatment produced a compact continuous scale whereas the CxPA scale was less compact and the NA left only discrete particles. This might suggest that aromatic acids with the COOH functionality on the ring are ineffective in forming this type of oxide scale. Both SEM and TEM examination of the scales before and after the challenge demonstrates that these initial scales were iron oxides that appear to be destroyed during the challenge with the formation of a thin sulfide layer (from the challenge acid) supported on residual pearlitic structures. Differences among the acid "protection" might be attributed to the time required for the challenge to break through the continuous oxide scales. EDS and XRD analysis on the TEM samples demonstrates that the oxide scale is composed of Fe_3O_4 (magnetite) that can be formed by the thermal decomposition of ferrous naphthenates. Metallurgy is also an important factor to promote the formation of the oxide scale, as evidenced by the fact that the oxide scale formed on 9Cr is more protective than that formed on CS. With PBA an oxide scale was still formed even at 288°C (550°F), although it was thinner than that formed at 316°C (600°F).

Future research will focus on further investigation on the effect of NAP structure, temperature and flow on the oxide scale formation.

REFERENCES

1. S.D. Kapusta, A. Ooms, A. Smith, F. Van den Berg, W. Fort, "Safe Processing of Acid Crudes," CORROSION/2004, paper no. 04637 (Houston, TX: NACE, 2004), p. 1.
2. E. Slavcheva, B. Shone, A. Turnbull, Review of Naphthenic Acid Corrosion in Oil Refining," *Brit. Corros. J.* 34, 2(1999): p. 125.
3. P. Jin, H.A. Wolf, and S. Nesic, "Analysis of Corrosion Scales Formed on Steel at High Temperatures in Hydrocarbons Containing Model Naphthenic Acids and Sulfur Compounds," *Surf. Interface Anal.* 47 (2015): p. 454.
4. F.X. Redl, C.T. Black, G.C. Papaefthymiou, R.L. Sandstrom, M. Yin, H. Zeng, C.B. Murray, S.P. O'Brien, "Magnetic, Electronic, and Structural Characterization of Nonstoichiometric Iron Oxides at the Nanolayer," *JACS* 126, 44 (2004): p. 14583.
5. ASTM G1 - 03 (2011), "Standard Practice for Preparing, Cleaning, and Evaluating Corrosion Test Specimens" (West Conshohocken, PA: ASTM).
6. S.G. Clarke, "The Use of Inhibitors (with Special Reference to Antimony) in the Selective Removal of Metallic Coatings and Rust," *Trans. Electrochem. Soc.* 69, 1 (1936): p. 131.

7. S. Stolen, R. Gloeckner, F. Gronvold, "Nearly Stoichiometric Iron Monoxide Formed as a Metastable Intermediate in a Two-Stage Disproportionation of Quenched Wüstite. Thermodynamic and Kinetic Aspects," *Thermochim. Acta* 256 (1995): p. 91